Comparative Study of Molecularly Imprinted Polymer and Magnetic Molecular Imprinted Nanoparticles as Recognition Sites for the Potentiometric Determination of Gemifloxacin Mesylate

Nehad A. Abdallah[1, 2,], Heba F. Ibhrahim[2], Nayira H. Hegabe[2]*

[1] Pharmacognosy and Pharmaceutical Chemistry Department, Faculty of Pharmacy, Taibah University, Al-Madinah Al-Mounawarah 41477, KSA
[2] Experiments and Advanced Pharmaceutical Research Unit, Faculty of Pharmacy, Ain Shams University, Cairo 1156, Egypt
[*]E-mail: nehad.amin@gmail.com

Two nanoparticles based potentiometric sensors were fabricated for the selective determination of gemifloxacin mesylate. The first sensor was based on the formation of molecularly imprinted polymer nanoparticles using methacrylic acid as a functional monomer, trimethylolpropane trimethacrylate as a crosslinker and azobisisobutyronitrile as the initiator. The second sensor was based on the use of Fe_3O_4 magnetic nanoparticles as core shells for the molecularly imprinted polymer. The developed sensors showed high selectivity, stability and sensitivity with wide concentration ranges of 1×10^{-3} - 1×10^{-8} mol L^{-1} and 1×10^{-3} - 1×10^{-10} mol L^{-1} for sensors 1 and 2, respectively. They were efficiently applied for the determination of gemifloxacin mesylate in bulk, pharmaceutical tablets and spiked human plasma.

1. INTRODUCTION

Gemifloxacin mesylate (GM), Fig.1, 7-[(4Z)-3-(Aminomethyl)-4-methoxyimino-pyrrolidin-1-yl]-1-cyclopropyl-6-fluoro-4-oxo-1,8-naphthyridine-3-carboxylic acid is a fourth generation antibacterial agent discovered in 1997 [1]. GM is characterized by its broad antibacterial activity against the gram-positive and gram-negative microorganisms. It is approved by FDA and used for the treatment of acute bacterial exacerbation of chronic bronchitis and community-acquired pneumonia caused by certain bacteria [2]. Several methods were applied for the determination of GM in bulk,

pharmaceuticals and biological samples such as spectrophotometry [3–6], spectrofluorimetry [7], HPLC [8–12], capillary electrophoresis [13–15], voltammetry [16–18], potentiometry [19,20].
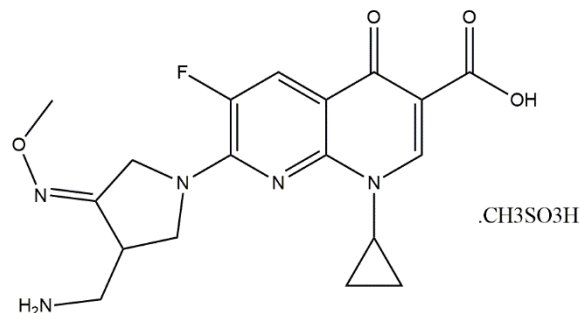
Figure 1. Chemical structure of gemifloxacin mesylate

The reported potentiometric methods were based on the formation of ion-pair complexes between GM and some ligands such as phosphotungstic acid, phosphomolybdic acid and ammonium reineckate. These reported electrodes exhibited narrow linearity ranges, limited stability and selectivity.

Molecularly imprinting polymer nanoparticles (MIP-NPs) can selectively recognize the target analyte based on the key to lock concept. The selective sorption and recognition of the template molecule is a result of the complementary conformations [21]. The polar functional groups in the template molecule allow the formation of more stable complexes when incorporated into a mixture of the functional monomer and the crosslinker that resulting in three-dimensional polymer structures [22].

The application of ion selective electrodes became a well-established technique in the routine pharmaceutical analysis. The use of MIP-NPs as recognition elements offers great advantages such as low-cost, high selectivity, better stability and ease of preparation. The high selectivity of MIP-NPs originated from their ability of the selective recognition of a target ion (template) by transferring it across the interface between the sample and the electrode paste [23].

The use of MIP-NPs, with all the advantages and progress that has been achieved, still face some challenges such as template leakage, slow mass transfer rate, limited binding capacity with difficult site accessibility. Some new techniques have been developed to solve these drawbacks. They include molecularly imprinted solid phase extraction, magnetic molecularly imprinted polymer with multi-walled carbon nanotubes and core-shell molecularly imprinted polymers [24].

Magnetic nanoparticles have been recently used. They promote the reaction between the MIP-NPs cavities and the analyte in the sample, which is due to the lower diffusion thickness layer compared to the bulk MIP-NPs and the high surface area to volume ratio. MIP with magnetic core provides regular shape with large surface area and allows active identification and dynamic separation [25].

The use of MMIP-NPs offers great advantages. They can exhibit a much higher specific recognition affinity, selectivity and capacity to the target molecule [26]. They can be used repeatedly with no significant decrease in its binding affinities [27]. MMIP-NPs are widely used in drug analysis and extraction procedures [28-31].

The aim of this research was the application of the molecularly imprinted technique for the first time in the determination of GM. Selectivity and sensitivity are considered as strong incentives to find new modifications for the development of electrochemical sensors. This was accomplished by using either MMIP-NPs or MIP-NPs as recognition sites and comparing their response characteristics in order to achieve higher stability, selectivity and sensitivity.

2. EXPERIMENTAL METHODS

2.1. Instrumentation

The potentiometric measurements were done using CLEAN digital ion analyzer PH 600, model 007747 (China) with constant stirring using Heidolph MR Hei-Standard, magnetic stirrer model 100818877. The electrodes potentials were measured versus Ag/AgCl double junction reference electrode, model Z113107-1EA batch 310 (Sigma-Aldrich). Malvern Zetasizer (United Kingdom) was used for particle size determination of the prepared nanoparticles. JEOL JEM-2100 Transmission Electron Microscope (Munchen, Germany) was used for imaging the nanoparticles.

2.2. Reagents

GM reference standard of potency 99.8% was kindly supplied by Mediphar Laboratories Dbayeh- Lebanon. Graphite powder and methacrylic acid (MAA) (Acros organics, USA). Trimethylolpropane trimethacrylate (TRIM) and azobisisobutyronitrile (AIBN) (Merck, Darmstadt, Germany). $FeCl_3.6H_2O$ and $FeCl_2.4H_2O$ (Fluka, USA). Hydroxyethylcellulose, oleic acid and paraffin oil (Prolabo, Pennsylvania, USA). All the used solvents were of analytical grade. Factive® tablets were purchased from the local market. It is manufactured by Tabuk Pharmaceutical Mfg. Co., Saudi Arabia, under license of LG Life Sciences.B.N. 5TW146.

2.3. Procedure

2.3.1. Preparation of Standard Solutions

The preparation process was conducted at room temperature. All the prepared solutions were stored at -5 °C when not in use. The GM standard aqueous solution of a concentration of 1×10^{-2} mol.L^{-1} was prepared in 250 mL volumetric flask, by weighing and dissolving 1.214 g GM in deionized water and the volume was completed to 250 mL with deionized water. Working standard solutions of different concentrations (1×10^{-3} to 1×10^{-11} mol.L^{-1}) were prepared by suitable dilution of the standard solution using deionized water.

2.3.2. Preparation of MIP-NPs

MIP-NPs were prepared by dissolving 1 mmol GM in 100 mL acetonitrile followed by the

addition of 10 mmol MAA. The mixture was sonicated for 5 min to allow prearrangement. Then, 17 mmol TRIM was added followed by 0.2 mmol AIBN. The resulting mixture was sonicated for 5 min and purged with N_2 gas for 15 min. The flask was sealed under this atmosphere to remove the dissolved O_2, which can inhibit the free radical polymerization. The flask was placed in a water bath at 70 °C for 24 h. After centrifugation, the polymer was washed with 200 mL of methanol and acetic acid (9:1 v/v %) for 20 h until no template detected by using UV spectrophotometry at 272 nm. The produced polymer was dried under vacuum at 40 °C for 24 h. NIP-NPs were produced under the same conditions without the addition of the template.

2.3.3. Preparation of Fe_3O_4 magnetic nanoparticles

A solution of 15 mmol $FeCl_3.6H_2O$ in deionized water was purged with nitrogen for 20 min and then 10 mmol $FeCl_2.4H_2O$ solution was added while mixing at 400 rpm in a 35°C water bath. The solution turned black by the addition of 5% ammonia solution dropwise at 800 rpm. The solution was kept in a 60°C water bath for 1 h with continuously purging with nitrogen. Nanoparticles of Fe_3O_4 were collected by external magnetic field. They were washed repeatedly with deionized water until the washing solution became neutral. The black Fe_3O_4 was dried under vacuum at 35°C for 12 h.

2.3.4. Preparation of MMIP-NPs

A mixture of 0.15 male AIBN, 5mmol TRIM and one-drop oleic acid was dissolved and mixed in 2 mL toluene. 100 mg of Fe_3O_4 nanoparticles were dissolved in 4 mL deionized water and added slowly to the oil phase. The mixture was stirred for 10 min followed by sonication for 5 min creating w/o emulsion. Three mmol MAA and 0.3 mmol GM were dissolved in 15 mL of 70% ethanol with continuous stirring. 25 mL of 0.4% hydroxyethyl cellulose was added to MAA solution followed by the dropwise addition of the prepared w/o emulsion with stirring at 300 rpm and purging of nitrogen gas at 70 °C for 24 h. The formed MMIP-NPs were collected by external magnetic field and washed with (Methanol: acetic acid) (9:1 % v/v) for 1 h followed by deionized water for 3 h. The MNIP-NPs were prepared in a similar way but without the addition of GM (template) molecule.

2.3.5. Preparation of nanoparticles based carbon paste electrodes

For the fabrication of carbon paste electrodes, 90 mg of graphite powder was homogenized in a mortar with 10 μl paraffin oil and 16 mg of MIP-NPs and MMIP-NPs nanoparticles separately. The Teflon cavity of the electrode was tightly filled with the produced paste. By pushing the steel screw forward through the electrode body, a new surface was obtained which was polished by a clean filter paper to get a new shiny surface.

2.4. Sensors Selectivity

The selectivity of the proposed sensors towards the interfering ions was determined by the calculation of the potentiometric selectivity coefficient using the separate solution method [32] by

applying the following equation

$$\log K_{A,B}^{pot} = \frac{(E_B - E_A) Z_A F}{(2.303 \, RT)} + \left(1 - \frac{Z_A}{Z_B}\right) \log[A] \quad \text{...............................} \quad (1)$$

Where $K_{A,B}^{pot}$ is the potentiometric selectivity coefficient. E_A is the potential measured for 1×10^{-4} mol L^{-1} GM solution, E_B is the potential measured for 1×10^{-4} mol L^{-1} interfering solution. Z_A and Z_B are the charges of GM and the interfering substance, respectively. $2.303RT/Z_AF$ is the slope of the calibration plot (mV/ concentration decade). [A] is the activity of GM.

2.5. Binding Study

Binding experiment was done by adding 20 mg of each of MIP-NPs and MMIP-NPs separately to 10 mL GM solutions of varying concentrations. The mixtures were kept under continuous stirring for 12 h at room temperature. The solid phase was separated by centrifugation at 3000 rpm for 10 min. The concentration of the free GM in the supernatant was detected by UV absorbance at 272 nm. The bound GM was calculated by subtracting the free GM concentration from the initial concentration. The obtained results were used for Scatchard analysis.

2.6. Determination of GM in bulk and pharmaceutical tablets

The electrochemical potential of GM was determined by the standard addition method [33]. The change in potential readings was recorded after the addition of a small volume of standard GM 1×10^{-2} mol.L^{-1} to 50 mL samples of different concentrations.

Twenty tablets of Factive® were accurately weighed, finely ground and mixed uniformly. An accurately weighed powder equivalent to 1.214 g GM was transferred to 250 mL volumetric flask. About 100 mL deionized water was added and the solution was sonicated for 10 min. The solution was filtered and completed to volume with deionized water. Several solutions of various concentrations ranging from 1×10^{-3} to 1×10^{-11} mol.L^{-1} were prepared by suitable dilutions of the prepared solutions. The solutions potentials were measured using the proposed sensors and the corresponding concentrations were calculated for each sensor from its specific regression equation.

2.7. Determination of GM in spiked human plasma

By the use of 5 mL volumetric flasks, 1.5 mL plasma was added and spiked with different volumes of the standard GM solution to provide different concentrations ranged from 0.05 to 6 µg.mL^{-1} which are equivalent to 1.03×10^{-7} to 1.2×10^{-5} mol L^{-1}. The volumes were completed to the mark using acetate buffer pH=4. The solutions were mixed with continuous shaking for 5 min. Then the solutions were transferred to 10 mL beaker for the potentiometric measurements using MMIP-NPs based sensor.

3. RESULTS AND DISCUSSION

3.1. Preparation of nanoparticles with different composition

MMIP-NPs were prepared by the classical co-precipitation method. Oleic acid was added as an emulsifier to facilitate the penetration of hydrophilic magnetic nanoparticles into the hydrophobic mixture of AIBN and TRIM. Hydroxyethylcellulose was used to improve the dispersion of Fe_3O_4 in the hydrophilic mixture of MAA and GM. Surface polymerization was carried out on Fe_3O_4 nanoparticles with MIP-NPs forming core-shell MIP-NPs. Hydrogen bond was formed when the template GM was added to MAA. Elution of GM from the prepared nanoparticles led to the creation of complementary cavities in the polymer matrix that acted as selective recognition sites. The amount of GM with MAA influenced the imprinting efficiency. Different molar ratios of the MAA and GM mixture were studied (2:1, 4:1, 8:1, 10:1, 12:1, 15:1) using UV spectrophotometry. It was found that the absorbance intensity increased with increasing MAA accompanied by a bathochromic shift up to molar ratio 10:1. The hydrogen bond was efficiently formed at this molar ratio; therefore, the ratio 10:1 was used in the formation of MIP-NPs and MMIP-NPs.

The crosslinker percentage affects the morphology of MIP-NPs and MMIP-NPs. High TRIM concentrations enhanced the polymers attachment causing blocking of the template recognition sites. Little concentrations led to an incomplete polymerization process which was concluded from the color of the produced polymer which was the same as naked black Fe_3O_4 particles. The molar ratio 5:3 of TRIM and MAA was sufficient for polymerization reaction and the resulting MMIP-NPs solution was brown in color.

3.2. Electrochemical response characteristics of the proposed sensors

Table 1. Electrochemical response characteristics of MIP-NPs and MMIP-NPs based sensors.

	Carbon Paste Electrodes	
	MIP-NPs Based Sensor	MMIP-NPs Based Sensor
Slope (mV/decade)[a]	53.5	59.8
LOD (mol L^{-1})[b]	3.6×10^{-9}	6.4×10^{-11}
Response time (s)	15	10
Working pH range	4.5 – 6	4 – 6
Concentration range (mol L^{-1})	1×10^{-8}-1×10^{-3}	1×10^{-10}-1×10^{-3}
Stability (days)	37	55
Average recovery%±SD[a]	97.46±0.36	99.21±0.48
Correlation coefficient	0.9993	0.9996
Repeatability (SD$_r$)	0.64	0.49
Intermediate precision	1.18	0.96
Ruggedness [c]	98.64±0.81	99.51±0.63

a Average of five determinations.

b Limit of detection (measured by the intersection of the extrapolated arms of the potential profile figures for each sensor)

c Average recovery percent of determining (10^{-5}, 10^{-4} and 10^{-3}M for the proposed sensors using Mettler Toledo MP225digital ion analyzer instead of clean PH 600 digital ion analyzer.

The electrochemical response characteristics are represented in table 1. MIP-NPs based sensor was fabricated by mixing the graphite powder with MIP-NPs and paraffin oil as a binder. MMIP-NPs based sensor was prepared by the addition of MMIP-NPs instead of MIP-NPs. By comparing the performances of the two sensors, it was found that the electrode behavior was greatly enhanced by the replacement of MIP-NPs with MMIP-NPs of the same mass, although MMIP-NPs contained much fewer recognition sites than MIP-NPs of the same amount. MMIP-NPs based sensor exhibited the best performance with a slope of 59.8 (mV/concentration decade) and a linear concentration range of 1×10^{-10} to 1×10^{-3} mol L^{-1}. MIP-NPs based sensor showed a smaller linear range from 1×10^{-8} to 1×10^{-3} mol L^{-1} with a Nernstian slope of 53.5 (mV/concentration decade). The potentiometric calibration profile of the studied sensors is represented in Fig.2.
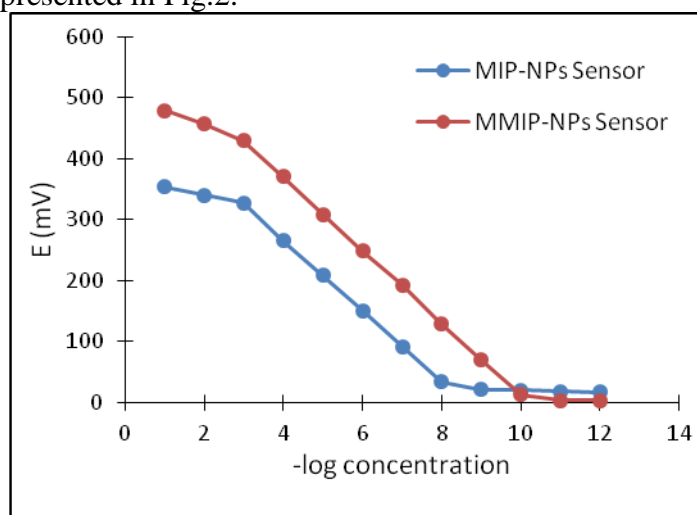

Figure 2. Potentiometric calibration profile of MIP-NPs and MMIP-NPs based sensors at 25°C.

Table 2. Comparison between the reported electrochemical methods and the studied sensors in GM determination

Method	Electrode	Linear range (mol L^{-1})	LOD (mol L^{-1})	Ref.
CV, DPV	B-cyclodextrin modified carbon paste electrode	$5\times10^{-8} - 2\times10^{-7}$	1.2×10^{-8}	[16]
CV, SWV, DPV	Multi-wall carbon nanotubes modified glassy carbon electrode	$5\times10^{-6} - 3\times10^{-5}$	1.85×10^{-9}	[17]
DPV, CV	Screen-printed carbon electrode	$0.5\times10^{-6} - 1\times10^{-5}$	0.15×10^{-6}	[18]
Potentiometry	PVC membrane with ammonium reineckate as ion exchanger	$1\times10^{-5} - 1\times10^{-2}$	1.1×10^{-6}	[19]
Potentiometry	CWEs with the ion-pairing phosphotungstic acid, phosphomolybdic acid and Ammonium reineckate.	$1\times10^{-7} - 1\times10^{-2}$	4.68×10^{-8}	[20]
Potentiometry	CPE modified with MIP-NPs	$1\times10^{-8} - 1\times10^{-3}$	3.6×10^{-9}	This work
Potentiometry	CPE modified with MMIP-NPs	$1\times10^{-10} - 1\times10^{-3}$	6.4×10^{-11}	This work

The superior response of the MMIP - NPs sensor may be explained by the effect of the

incorporation of Fe_3O_4 nanoparticles in the enhancement of the electrochemical response. The negative effect of MIP-NPs on the electron transfer rate between the target analyte and the electrode surface is mainly due to the insulating property of MIP-NPs [34]. This effect can be minimized by the use of magnetic nanoparticles. Fe_3O_4 nanoparticles can improve the stability of the sensor and the electron transfer rate of the electrochemical reaction. They provide high surface area, enhance the mass transfer and improve the binding affinity to the template. This leads to decrease in the binding time and the diffusion layer. The lower stability and sensitivity of MIP-NPs based sensor may be attributed to the insulating effect of MIP-NPs and the agglomeration of MIP-NPs when becoming in contact, which may lead to decrease the availability of recognition sites. A comparison between the studied sensors and other reported electrochemical sensors is represented in table 2. It revealed the superiority of the proposed MIP-NPs and MMIP-NPs based sensors on the determination of GM with high sensitivity, stability and accuracy.

3.3. FTIR analysis

The FTIR spectrum of the prepared nanoparticles is represented in Fig.3. In the case of MIP-NPs and NIP-NPs, both polymers have similar FTIR spectra indicating the similarity in their backbone structure. They revealed the peaks of the OH of COOH group at 3490 cm^{-1}, carbonyl group stretching vibration at 1760 cm^{-1} and C-H vibrations at 2920, 1450, 1300, 780 cm^{-1}. The peaks of MIP-NPs are relatively sharper than that of NIP-NPs. GM was effectively leashed from MIP-NPs, which was confirmed by comparing with NIP-NPs. No residue of GM molecules was detected.
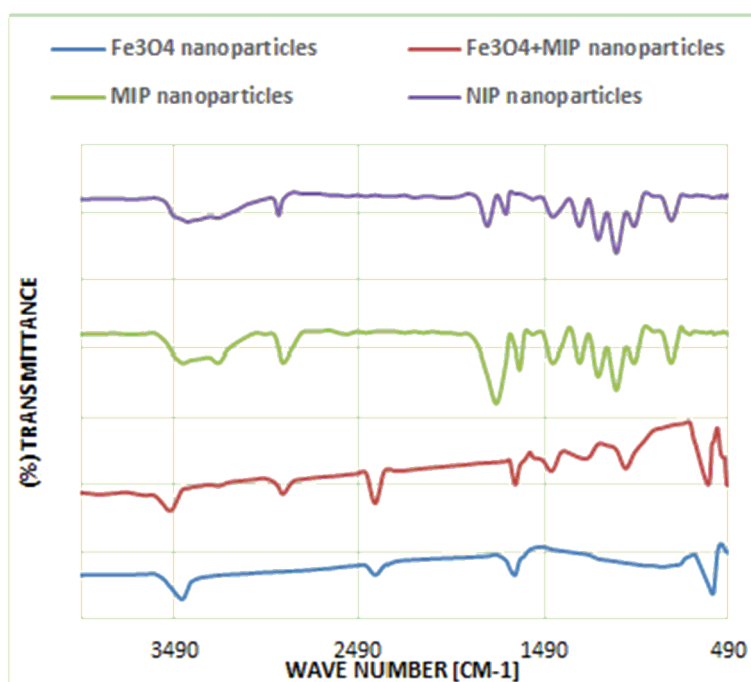

**Figure 3.** FTIR spectra of Fe_3O_4 nanoparticles, MMIP, MIP and NIP nanoparticles.

By comparing the FTIR spectrum of Fe_3O_4 to that of the MMIP-NPs, it was found that the Fe_3O_4 nanoparticles revealed Fe-O bond at 580 cm^{-1}. This bond was also found in MMIP-NPs. It indicated that Fe_3O_4 was embedded into MIP-NPs. MMIP-NPs revealed the peaks of C=O at 1650 cm^{-1}, the one of the C-O-C at 1200 cm^{-1} and the peaks at 2900, 3500 cm^{-1} related to C-H and OH of COOH, respectively. All these peaks indicated the formation of a polymer shell consisted of MAA and TRIM around Fe_3O_4 nanoparticles.

3.4. Particle size analysis

Particle size distribution of the prepared nanoparticles was studied by Zeta-sizer as shown in Fig.4. The mean particle size of Fe_3O_4 nanoparticles was found to be 20 nm ranged from (8-25nm), while that of MIP-NPs and MMIP-NPs were found to be 80 (30-110 nm) and 50 (25-80 nm), respectively. The increment of the size of Fe_3O_4 in MMIP-NPs is due to the uniform MIP-NPs coating. There were no free MIP-NPs found in TEM. TEM images of the prepared nanoparticles in Fig.5 showed their uniform spherical shapes with relatively narrow particle size distribution.
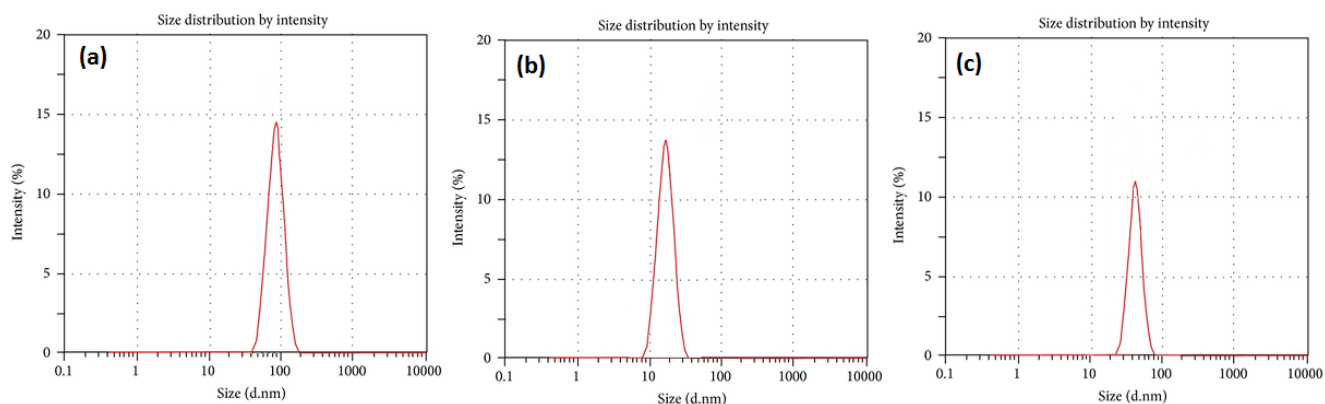
Figure 4. Particle size analysis record by zeta-sizer of (a) MIP-NPs, (b) Fe_3O_4-NPs and (c)MMIP-NPs.
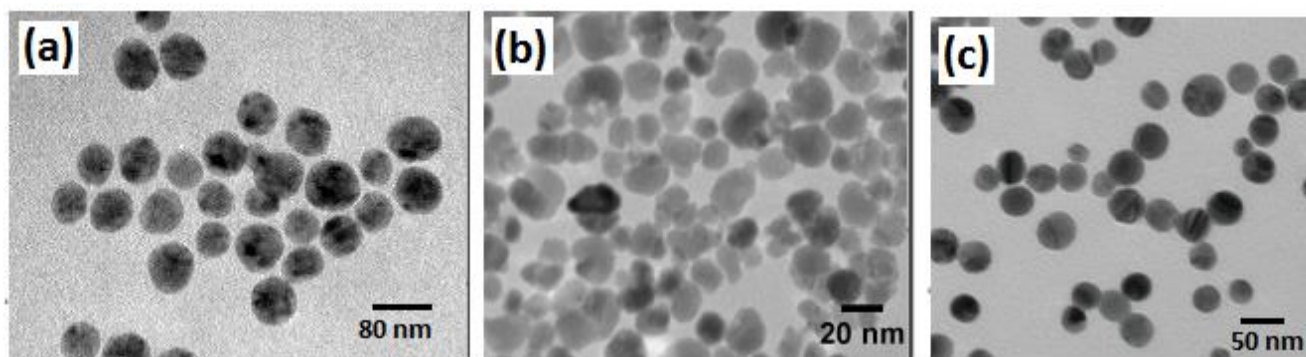
Figure 5. TEM images of (a) MIP-NPs, (b) Fe_3O_4-NPs and (c)MMIP-NPs.

3.5. Binding Characteristics of the magnetic molecularly imprinted nanoparticles

When a GM solution presents in direct contact with MIP-NPs and MMIP-NPs, it interacts with

the binding sites of the solid adsorbents. Adsorption isotherm is an important tool to understand the way of interaction of GM molecules with the adsorbent surfaces, the binding mechanism and the binding sites distributions in the interaction.

This was done by plotting the binding capacity (Q) versus the free ligand in the liquid phase. Q was calculated using the following equation:

$$Q = \frac{(C_i - C_f)V_s}{M} \times 1000 \dots\dots\dots\dots\dots\dots\dots\dots\dots\dots\dots (2)$$

Where Q is the binding capacity of either MIP-NPs or MMIP-NPs ($\mu mol.g^{-1}$). C_i is the initial GM concentration ($\mu mol.mL^{-1}$). C_f is the final GM concentration ($\mu mol.mL^{-1}$). Vs is the volume of the solution (mL). M is the mass of the dried polymer.

As shown in Fig.6, the binding capacity of MIP-NPs and MMIP-NPs increased with increasing the initial ligand concentration and reaching saturation at higher concentrations.

It was found that MMIP-NPs required higher concentrations for saturation compared to MIP-NPs. This means that MMIP-NPs displayed a higher affinity for the ligand other than MIP based one.

The binding parameters for all the studied nanoparticles were calculated by Scatchard analysis using the following equation:

$$\frac{Q}{C\ free} = \frac{Q\ max - Q}{Kd} \dots\dots\dots\dots\dots\dots \dots\dots\dots\dots\dots (3)$$

Where Q, is the binding capacity. Cf_{ree} is the free GM concentration at equilibrium. Q_{max} is the maximum apparent binding capacity. K_d is the dissociation constant at the binding sites. The equilibrium dissociation constant was calculated from the slope and the apparent maximum number of binding sites from the y-intercepts in the linear plot of Q/C_{free} vs. Q.
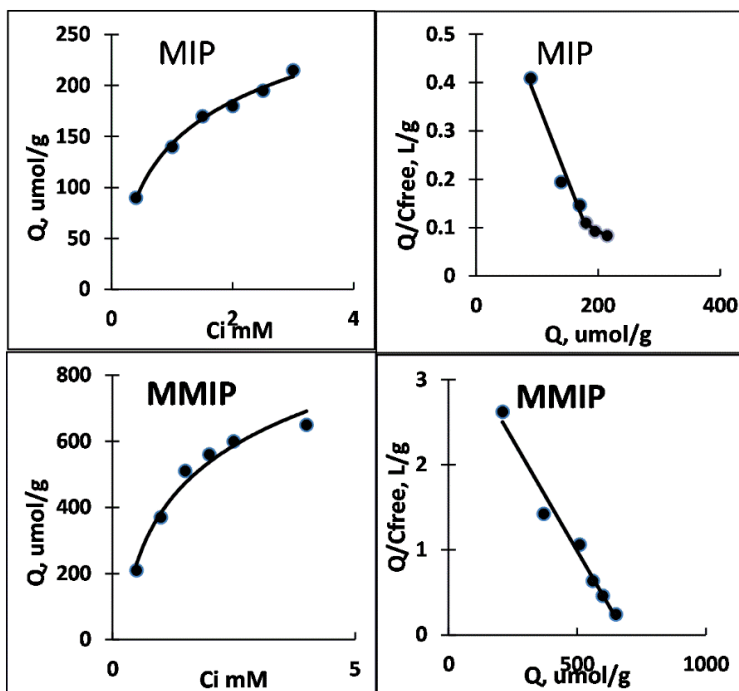
Figure 6. Binding isotherms and scatchard plots for MIP-NPs and MMIP-NPs.

It was found that the Scatchard plot of MIP-NPs was not linear. It showed two distinct sections

which mean that the binding sites are not uniform and represent two different classes of binding sites of either high or low affinity. The apparent K_d for high and low-affinity binding sites were 303 and 1428.5 µmol/l accompanied with site population of 208.3 and 341 µmol/g for the dry polymer, respectively. In the case of MMIP-NPs, the Scatchard plot was linear in all concentration ranges. This suggested that the binding sites were of one type, selective and homogeneous. The apparent K_d was 192.31 µmol/l accompanied with site population of 692.04 µmol/g. These results proved the decrease in the recognition ability of MIP-NPs relative to MMIP-NPs, which may be due to the agglomeration of MIP-NPs as described previously.

3.6. Life span of the proposed sensors

Table 3. Electrochemical response of the MIP-NPs and MMIP-NPs based sensors during their lifetime at 25°C.

Electrode composition	Soaking time	Slope (mV/decade)	Usable concentration range (mol L^{-1})	Response time (s)
	0.5 h	52.6	1.0×10^{-8} - 1.0×10^{-3}	18
	1 h	53.5	1.0×10^{-8} - 1.0×10^{-3}	18
CPE 1	2 h	50.34	1.0×10^{-8} - 1.0×10^{-3}	17
90 mg	12 h	55.67	1.0×10^{-8} - 1.0×10^{-3}	15
graphite	24 h	53.6	1.0×10^{-8} - 1.0×10^{-3}	15
powder + 16	6 days	53.8	1.0×10^{-8} - 1.0×10^{-3}	16
mg MIP-NPs	11 days	53.2	1.0×10^{-8} - 1.0×10^{-3}	17
+ 10 µl	28 days	52.6	1.0×10^{-8} - 1.0×10^{-3}	15
paraffin oil	37 days	53.8	1.0×10^{-8} - 1.0×10^{-3}	15
	53 days	48.2	1.0×10^{-7} - 1.0×10^{-4}	20
	65 days	46.4	1.0×10^{-6} - 1.0×10^{-4}	22
	0.5 h	59.3	1.0×10^{-10} - 1.0×10^{-3}	10
	5 h	58.6	1.0×10^{-10} - 1.0×10^{-3}	9
CPE 2	10 h	59.5	1.0×10^{-10} - 1.0×10^{-3}	10
90 mg	18 h	58.5	1.0×10^{-10} - 1.0×10^{-3}	8
graphite	2 days	59.6	1.0×10^{-10} - 1.0×10^{-3}	9
powder + 16	12 days	59.8	1.0×10^{-10} - 1.0×10^{-3}	9
mg MMIP-	20 days	60.2	1.0×10^{-10} - 1.0×10^{-3}	10
NPs + 10 µl	33 days	59.7	1.0×10^{-10} - 1.0×10^{-3}	9
paraffin oil	55 days	59.2	1.0×10^{-10} - 1.0×10^{-3}	9
	64 days	52.8	1.0×10^{-9} - 1.0×10^{-3}	15
	70 days	50.7	1.0×10^{-9} - 1.0×10^{-4}	25

The electrode lifetime is the period in which the electrode is optimally functioning until at least one of the performance characteristics deviates from its ideal value. With all the studied sensors, the response time, LOD, linear range and calibration slope were continuously measured to ensure their reproducibility within ± 2 % of the original values. The slope values of the proposed sensors started to deviate from its value by 10 % after 37 and 55 days for MIP-NPs and MMIP-NPs sensors, respectively as represented in table 3. These data were based on using the same electrode without any surface

renewal.

3.7. Dynamic response time of the proposed sensors

The practical response time required to reach 90% of the maximum potential or to achieve a steady potential response (± 2 mV) was evaluated by a 10-fold increase in GM concentration. It was found that the response time of the proposed sensors was 15 and 10 s for MIP-NPs and MMIP-NPs based sensors, respectively. The responses of the electrodes did not change by measuring the concentrations of GM either starting from high to low or from low to high concentrations as represented in Fig.7. This approves the reversibility of the studied electrodes, although the time required to reach the equilibrium values from high to low measurements was longer than that for measuring the concentrations from low to high.
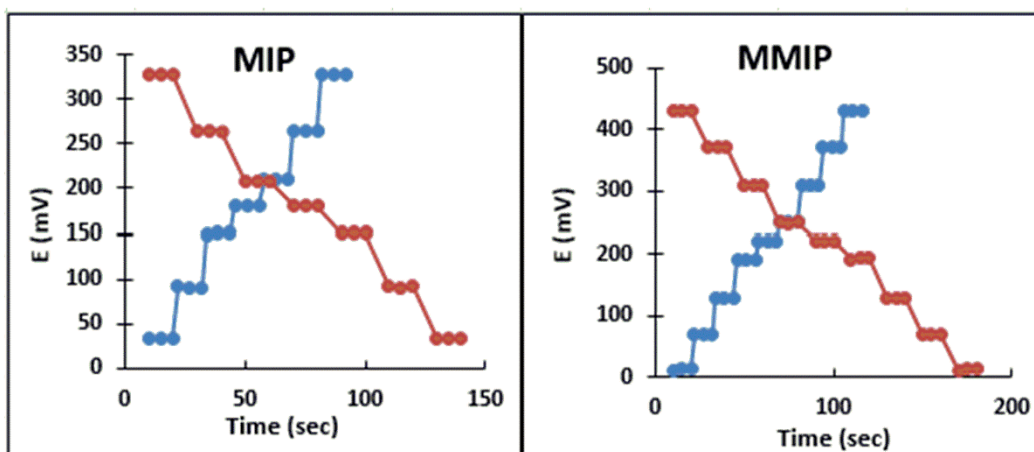

Figure 7. Dynamic response time of MIP-NPs and MMIP-NPs based sensors from high to low and from low to high concentrations at 25°C.

3.8. Effect of pH

A carboxylic group and an amino group are two ionizable functional groups that characterize Fluoroquinolones. GM carries a carboxylic group (pka= 6.05) and primary amino group (pka=8.93) [2]. According to the pH of the medium, GM can be present in four forms: anionic, zwitterionic, neutral non-ionized and cationic. In a strongly acidic medium, only the amino group is positively charged. In a strongly alkaline medium, only the 3-carboxylic group is negatively charged. In neutral pH, the amphiprotic form predominates. Therefore, the pH of the measured solution is an important factor in the potentiometric measurements. The pH effect on the sensors' responses was studied over the pH range from 2 to 10. The potentials of the electrodes did not change over the range 3 to 4.5 as shown in Fig.8. Non-Nernstian slopes were observed below and above this range. This may be attributed to the presence of several isoforms of GM, presenting different charges and concentration levels. The Nernstian response over the pH range from 3 to 4.5 is mainly due to the existence of the cationic form. Therefore, acetate buffer of pH 4 was used as the most appropriate pH for more

electrochemical investigation.
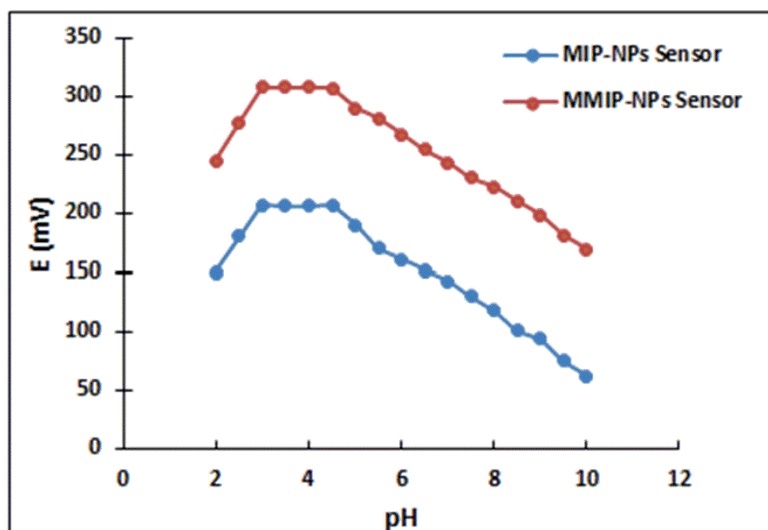
Figure 8. Effect of pH on the potentiometric response of MIP-NPs and MMIP-NPs based sensors at 25°C.

3.9. Selectivity coefficients of the proposed sensors

Table 4. Selectivity coefficients of the proposed MIP-NPs and MMIP-NPs based sensors with some interfering and structurally related ions using separate solution method.

Interferents	$-\log K^{pot}_{GM, interferent}$	
	MIP-NPs Based Sensor	MMIP-NPs Based Sensor
Na^+	4.5	5.81
Li^+	5.43	6.11
Ca^{2+}	3.23	4.12
Mg^{2+}	3.15	3.89
Cu^{2+}	4.34	4.9
Glucose	4.32	3.78
Lactose	5.03	4.67
Warfarin	5.18	5.89
Theophylline	4.55	5.38
Omeprazole	4.38	5.13
Moxifloxacin	3.45	4.38
Pazufloxacin	4.78	4.16
Levofloxacin	4.68	3.78
Ciprofloxacin	4.23	5.34

The selectivity of the proposed sensors was measured relative to other interfering ions using the separate solution method. The results were represented in table 4. It was found that all the proposed sensors were highly sensitive and selective for GM in the presence of either interfering cations, co-

administered drugs or structurally related fluoroquinolones. This may be attributed to the existence of a selective binding to the imprinted cavities of MIP-based sensors resulting from the hydrogen bonding between the template and the functional monomers. Such the functional monomer may form hydrogen bonds with several moieties of GM such as fluorine, primary and tertiary amino groups and the carboxyl group. TRIM, the crosslinker allowed the production of a rigid polymer possessing stable binding cavities for the template molecule.

3.9. Analytical applications

Table 5.. Determination of GM by applying the standard addition method and statistical comparison with a reported method for GM determination

	MIP-NPs Sensor			MMIP-NPs Sensor		
	Taken $(mol\ L^{-1})$	Recovery %	RSD	Taken $(mol\ L^{-1})$	Recovery %	RSD
Pure solution	3×10^{-4}	99.65	0.48	5×10^{-4}	98.79	0.79
	1×10^{-5}	98.48	0.87	4×10^{-6}	100.13	0.87
	8×10^{-5}	100.03	0.65	5×10^{-5}	98.67	0.59
	4×10^{-6}	99.37	1.02	3×10^{-7}	100.02	1.02
	5×10^{-7}	100.12	0.66	7×10^{-9}	99.39	0.88
Average± SD		99.53 ± 0.66			99.40 ± 0.67	
n		5			5	
Variance		0.44			0.45	
F-test (5.19)[a]		2.51			2.45	
Student t test (2.262)[a]		0.96			0.77	
Factive Tablet® (320 mg gemifloxacin)	5×10^{-4}	98.69	1.02	5×10^{-4}	100.17	0.85
	9×10^{-4}	99.54	0.96	4×10^{-6}	99.69	1.03
	3×10^{-5}	98.79	0.77	8×10^{-7}	98.57	1.16
	1×10^{-6}	99.28	0.56	2×10^{-8}	98.43	0.93
	1×10^{-7}	100.67	0.91	5×10^{-9}	99.72	0.87
Average± SD		99.39 ± 0.79			99.32 ± 0.77	
n		5			5	
Variance		0.62			0.59	
F-test (5.19)[a]		2.17			2.28	
Student t test (2.262)[a]		0.037			0.029	

a The values into parentheses are the corresponding theoretical values of t and F at the 95% confidence level.

N.B.: The reported method [3] average recovery ± SD (99.56 ± 1.05), n=6 for pure solution and (100.87 ± 1.16), n=6 for pharmaceutical dosage form

The determination of GM in bulk and Factive® tablets was performed by the use of the proposed sensors. As shown in table 5, the results revealed the applicability of the sensors for the determination of GM with high accuracy, precision and recovery. The results of the sensors were

statistically compared with one of the reported methods [3] using t-test and F-test. They showed no significant difference between the studied electrodes and the reported method.

The studied MMIP-NPs based electrode was effectively used in the determination of GM in spiked human plasma with high recovery and accuracy as shown in table 6. This was done without either the need of a preliminary sophisticated extraction procedure or the use of expensive instruments.

Table 6. Accuracy and precision of GM in spiked human plasma.

|	Plasma concentration ($\mu g.mL^{-1}$)	Calculated mean plasma concentration ($\mu g.mL^{-1}$)*	SD[a]	CV% [b]	Recovery %	RE%[c]
Intra-day	0.08	0.080	0.0019	2.40	100.25	-0.25
	0.25	0.249	0.0053	2.12	99.52	0.48
	0.5	0.490	0.0187	3.82	98.00	2.00
	1	0.996	0.0197	1.98	99.64	0.36
	2.5	2.498	0.0295	1.18	99.92	0.08
	4	4.012	0.0606	1.51	100.30	-0.30
	5.5	5.468	0.1188	2.17	99.42	0.58
Inter-day	0.08	0.079	0.0067	8.39	99.17	0.83
	0.25	0.247	0.0015	0.62	98.67	1.33
	0.5	0.509	0.0115	2.27	101.80	-1.80
	1	0.985	0.0050	0.51	98.47	1.53
	2.5	2.483	0.0252	1.01	99.33	0.67
	4	3.933	0.0404	1.03	98.33	1.67
	5.5	5.503	0.0252	0.46	100.06	-0.06

* Average of five determinations

a: SD: standard deviation

b:CV%: coefficient of variation%

c: RE%: relative error %

The MIP-NPs based sensor was effectively used for the quantitative determination of the dissolution profile of one 320mg gemifloxacin (Factive®) tablet. 900 mL of 0.1 N HCl was prepared and used as the dissolution medium that maintained at 37°C ± 5 at 50 rpm for 45 min. The amount of GM released at different time intervals was potentiometrically measured by MIP-NPs based sensor. The release profile of GM at different time intervals is represented in Fig.9. The effectiveness of the pharmaceutical tablets relies on the drug dissolution in the GIT fluids prior to its absorption into the systemic circulation. It is used as a routine assessment of the product quality and prediction of the in-vivo availability. The dissolution profile of Factive® tablets revealed that more than 70% of the drug was dissolved within 45 min. According to FDA, this result can ensure that the bioavailability of the drug is not limited by its dissolution; the rate-limiting step for the drug absorption is gastric emptying [35].
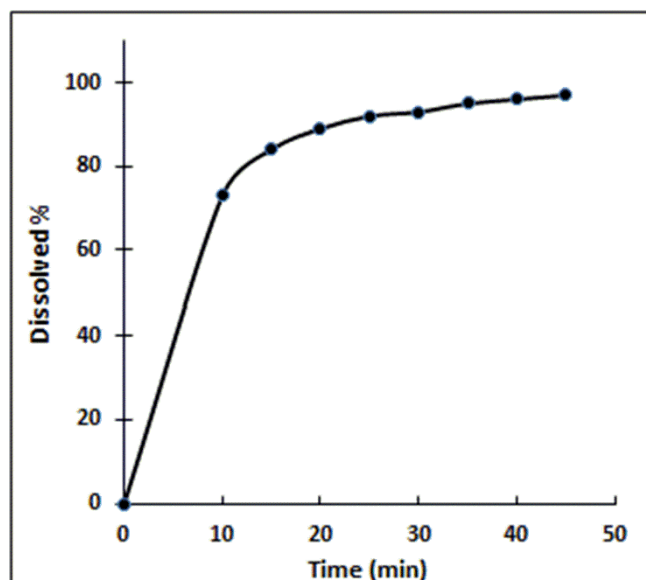
Figure 9. Dissolution profile of gemifloxacin mesylate tablet at 37 °C.

4. CONCLUSION

The use of Fe_3O_4 magnetic nanoparticles as core shells for MIP-NPs was effective as recognition elements in the selective potentiometric determination of GM with high accuracy, wide linear range and high sensitivity. They were applied for the determination of GM in bulk, pharmaceutical tablets and spiked plasma samples. In comparison with MIP-NPs, the MMIP-NPs based sensor showed wider linearity concentration range, higher stability, shorter response time and higher sensitivity that reached Pico-gram level. The MMIP-NPs sensor was used efficiently in the determination of GM in human plasma samples with the acceptable degree of accuracy and precision.

References

1. C.Y. Hong, Y.K. Kim, J.H. Chang, S.H. Kim, H. Choi, D.H. Nam, Y.Z. Kim and J.H. Kwak, *J. Med. Chem.,* 2623 (1997) 3584.
2. J.A. Goswami and N.J. Shah, *Int. J. Pharm. Pharm. Sci.,* 5 (2013) 931.
3. S. Dey, Y.V. Reddy, B. Krishna, S.K. Sahoo, P.N. Murthy, D. Kumar, J. Alam and M. Ghosh, *Int. J. Chem. Anal. Sci.*, 1 (2010) 130.
4. M.V. Krishna and D.G. Sankar, *E-J Chem.*, 5 (2008) 515.
5. S. Sahu, S.K. Patro, U.L. Narayan and B. Garnaik, *Pharm. Methods,* 3 (2012) 26.
6. D. Zidan, O.A. Ismaiel, W.S. Hassan and A. Shalaby, *J. Appl. Pharm. Sci.,* 6 (2016) 136.
7. S. Evrim, K. Tekkeli and A. Onal, *J. Fluores.c,* 21 (2011) 1001.
8. N. A Abdallah, *J. Chromatogr. Sep. Tech.,* 5 (2014) 1.
9. B.M.H. Al-hadiya, A.A. Khady and G.A.E. Mostafa, *Talanta*, 83 (2010) 110.
10. M. Kaiser, L.D. Grünspan, T. Dalla and L. Tasso, *J. Chromatogr.* B, 879 (2011) 3639.
11. R.N. Rao, C. Gangu, K.G. Prasad and R. Narasimha, *Biomed. Chromatogr.,* 25 (2011) 1222.
12. B. Roy, A. Das, U. Bhaumik, A.K. Sarkar, A. Bose, J. Mukharjee, U.S. Chakrabarty, A.K. Das and T.K. Pal, *J. Pharm. Biomed. Ana.*, 52 (2010) 216.

13. A.A. Elbashir, B. Saad, A. Salhin, M. Ali and K.M.M. Al-azzam, *J. Liq. Chromatogr. Relat. Technol.,* 31 (2008) 1465.
14. S. Il, J. Shim, M. Kim, Y. Kim and D. Soo, *J. Chromatogr. A,* 1055 (2004) 241.
15. E. Kim, Y. Koo and D. Soo, *J. Chromatogr. A,* 1045 (2004) 119.
16. M.A. El-shal, A.K. Attia and S.A. Abdulla, *J. Adv. Sci. Res.*, 4 (2013) 25.
17. R. Jain and J.A. Rather, *Colloid Surface B*, 83 (2011) 340.
18. A. Radi, A. Khafagy, A. El-shobaky and H. El-mezayen, *J. Pharm. Anal.,* 3 (2013) 13.
19. N.F. Abo-talib, *Anal. Bioanal. Electrochem.*, 5 (2013) 74.
20. A.M. Al-mohaimeed, S.A. Al-tamimi, N.A. Alarfaj and F.A. Aly, *Int. J. Electrochem. Sc.,* 7 (2012) 12518.
21. S. Li, X. Huang, M. Zheng, W. Li and K. Tong, *Sensors,* 8 (2008) 2854.
22. S.A. Zaidi and J.H. Shin, *Int. J. Electrochem. Sc.,* 9 (2014) 4598.
23. M. Javanbakht, B. Akbari-Adergani, Molecularly Imprinted Sensors, *Elsevier* B.V, 2012, Oxford, UK.
24. A. Saeedeh and K. Majid, *Talanta*, 167 (2017) 470.
25. X. hong Gu, R. Xu, G. lin Yuan, H. Lu, B. ren Gu and H. ping Xie, *Anal. Chim. Acta,* 675 (2010) 64.
26. A.K. Mohammad, R. Mehdi and B. Zohrel, *Inorganic and Nano-Metal Chemistry,* 47 (2017) 308.
27. S. Golaleh, H. Moayad, K. Salah, S. Mirabdollah and A. Awat, *J. Chromatogr. B*, 1011 (2016) 1.
28. J. Ding, F. Zhang, X. Zhang, L. Wang, C. Wang, Q. Zhao, Y. Xu, L. Ding and N. Ren, *J. Chromatogr. B*, 1021 (2016) 221.
29. A. Ait Lahcena, A.A. Baleg, P. Baker, E. Iwuoha and A. Amine, *Sensor Actuat. B*, 241 (2017) 698.
30. W. Zhu, L. Xu, C. Zhu, B. Li, H. Xiao, H. Jiang and X. Zhou, *Electrochim. Acta,* 218 (2016) 91.
31. G. Sheykhaghaei, M. Hossaini-Sadr and S. Khanahmadzadeh, *Bull. Mater. Sci.,* 39 (2016) 647.
32. Y. Umezawa, P. Bühlmann, K. Umezawa, K. Tohda and S. Amemiya, *Pure Appl. Chem.*, 72 (2000) 1851.
33. E.W. Baumann, *Anal. Chim. Acta*, 42 (1968) 127.
34. T. Alizadeh and S. Azizi, *Biosens. Bioelectron.*, 81 (2016) 198.
35. Guidance for Industry, Dissolution Testing of Immediate Release Solid Oral Dosage Forms, U.S. Department of Health and Human Services, *Food and Drug Administration Center for Drug Evaluation and Research (CDER),* (2015).